S©MR ISSN 1813-3304

СИБИРСКИЕ ЭЛЕКТРОННЫЕ
МАТЕМАТИЧЕСКИЕ ИЗВЕСТИЯ

Siberian Electronic Mathematical Reports

http://semr.math.nsc.ru

Том 18, №2, стр. 1238–1250 (2021) УДК 519.63
DOI 10.33048/semi.2021.18.094 MSC 65M08

THE ACCURACY OF NUMERICAL SIMULATION OF THE ACOUSTIC WAVE PROPAGATIONS IN A LIQUID MEDIUM BASED ON NAVIER-STOKES EQUATIONS

A.S. KOZELKOV, O.L. KRUTYAKOVA, V.V. KURULIN,
D.YU. STRELETS, M.A. SHISHLENIN

Abstract. The space and time resolution needed to simulate the propagation of acoustic perturbations in a liquid medium is estimated. The dependence of the solution accuracy on the parameters of an iterative procedure and a numerical discretization of the equations is analyzed. As a numerical method, a widely used method called SIMPLE is used together with a finite-volume discretization of the equations. A problem of propagation of perturbations in a liquid medium from a harmonic source of oscillations is considered for the estimation. Estimates of the required space and time resolution are obtained to provide an acceptable accuracy of the solution. The estimates are tested using the problem of propagation of harmonic waves from a point source in a liquid medium.

Kozelkov, A.S., Krutyakova, O.L., Kurulin, V.V., Strelets, D.Yu., Shishlenin, M.A., The accuracy of numerical simulation of the acoustic wave propagations in a liquid medium based on Navier-Stokes equations.

The work of A.S. Kozelkov and M.A. Shishlenin was supported by RSCF under grant 19-11-00154 “Developing of new mathematical models of acoustic tomography in medicine. Numerical methods, HPC and software”. The work of A.S. Kozelkov and D.Yu. Strelets was supported by the Program for Creation and Development of World-Class Scientific Center “Supersonic” in 2020-2022 with financial support of the Russian Ministry of Education and Science (Agreement № 075-15-2020-924 dated 16.11.2020). The results of A.S. Kozelkov, O.L. Krutyakova and V.V. Kurulin have been obtained with financial support from the Science & Universities National Project under the Young Scientists Lab Program of the RF Ministry of Education and Science (Research Topic: Development of CFD methods, models and algorithms to simulate liquids and gases in natural and industrial environments under normal and critical conditions on petascale supercomputers).

Received October, 5, 2021, published November, 17, 2021.

Keywords: hydroacoustics, numerical simulation, Navier-Stokes equations, method SIMPLE, finite-volume discretization, numerical dissipation, Logos software package, acoustic tomography.

1. Introduction

An important problem in fluid dynamics is simulating the phenomena of generation and propagation of acoustic waves in a liquid medium [1, 2]. Such problems arise in medicine acoustic tomography [25, 27, 28, 29], simulating the rotation of propeller engines to decrease the generated noise level [3] and flows in the elements of reactor units to study the interaction of noise of turbulent structures with the structural elements of the units [4], etc. Currently, a three-dimensional numerical simulation method based on solving the Navier-Stokes equations is widely used to simulate the above problems [5, 6]. This approach allows describing the process of generation and propagation of acoustic waves by taking into account the unsteady processes of turbulent mixing. A popular approach to numerically solving the Navier-Stokes equations for incompressible and weakly compressible fluids is a finite-volume discretization in space together with an iterative method called SIMPLE [7, 8] or its modifications [9, 10].

Numerical solution of systems of PDE is widely used for hydroacoustics problems. For instance, in [**?**, 30, 32] the 2D application to acoustic tomography based on the system of linear hyperbolic equations is considered. The problem of modelling of radiation patterns of sources was considered in [35]. The method of recovering the initial state of a supernova is proposed [31]. The article [11] deals with flows passing by bodies that create pressure pulsations and generate acoustic waves, as well as the influence of the shape of bodies on the frequency, amplitude and nature of the signal. The acoustic oscillations in the near field are described by solving the Navier-Stokes equations, and the propagation of noise in the far field, by integral methods. In [12], the parameters of noise propagation are estimated for flows past a square cylinder. The influence of the aspect ratio of the body shape is considered by using the compressible Navier-Stokes equations and high-order accurate schemes. In [13], some modifications of the airfoil geometry and their influence on noise propagation and dissipation are investigated, and the Navier-Stokes equations, with an integral analogy, are solved in the near field. Although this approach is widely used, the dependence of the accuracy of simulation of the propagation of acoustic perturbations in a liquid medium on the space and time resolution, the peculiarities of discretization, and the parameters of the iterative process has been poorly studied. Therefore, estimating the accuracy of simulation of the propagation of acoustic perturbations in a liquid medium is an important problem.

The purpose of this paper is to estimate the space and time resolution needed in simulating the propagation of acoustic perturbations in a liquid medium and analyze the dependence of the solution accuracy on the parameters of the iterative procedure and the numerical discretization used for the equations. In this study, the SIMPLE method is implemented with a software package called LOGOS. The software implementation of the method has been validated and tested on various classes of problems [14, 15, 16, 17, 18]. The numerical discretization is based on a finite volume method and second-order accurate schemes for the space and time terms. The finite propagation speed of an acoustic wave is taken into account by using an equation of state for a liquid with a nonzero compressibility coefficient.

Finite difference schemes providing an improved representation of a range of scales (spectral-like resolution) in the evaluation of first, second, and higher order derivatives were presented and compared with well-known schemes [24]. Schemes were also presented for derivatives at mid-cell locations, for accurate interpolation and for spectral-like filtering and discussed for applications of fluid mechanics.

In this study, a problem of propagation of perturbations in a liquid medium from a harmonic source of oscillations is solved, and the resulting wave pattern is compared with an analytical solution and a measured wave diffusion coefficient. This paper presents estimates of the acceptable grid sizes, the time step, and the number of iterations per step expressed in terms of dimensionless parameters with respect to the wave parameters needed to guarantee the required accuracy of the solution of the hydroacoustic problems. The effects of the discretization schemes for the convective and transient terms and the number of internal iterations per step on the solution accuracy are estimated.

The results presented in this paper are typical for most hydrodynamic finite-volume codes and can be used in solving many hydroacoustics problems.

2. Mathematical model and numerical method

The unsteady three-dimensional isothermal flows of a viscous compressible fluid are described by a system of Navier-Stokes equations containing a continuity equation and a momentum conservation equation [5] supplemented by an equation of state. In conservative form and in Cartesian coordinates, the equations may be written as follows:

$$\frac{\partial \rho}{\partial t} + \frac{\partial}{\partial x_i}(\rho \mathbf{u}_i) = 0, \tag{1}$$

$$\frac{\partial (\rho \mathbf{u}_i)}{\partial t} + \frac{\partial}{\partial x_j}(\rho \mathbf{u}_i \mathbf{u}_j) = -\frac{\partial p}{\partial x_i} + \frac{\partial}{\partial x_j}\tau_{ij}, \tag{2}$$

$$\rho = \rho(p). \tag{3}$$

Here t is the time variable, $\mathbf{u}_i = \{u_1, u_2, u_3\} = \{u, v, w\}$ is the velocity, ρ is the density, p is the pressure, and τ_{ij} is the viscous stress tensor:

$$\tau_{ij} = \mu\left(\left(\frac{\partial \mathbf{u}_i}{\partial x_j} + \frac{\partial \mathbf{u}_j}{\partial x_i}\right) - \frac{2}{3}\frac{\partial \mathbf{u}_k}{\partial x_k}\delta_{ij}\right). \tag{4}$$

Here μ is the molecular dynamic viscosity. The relation between the pressure and density is determined by the equation of state $\rho = \rho_0 + k(p - p_0)$, where k is the compressibility coefficient, ρ_0, p_0 is the basic density and pressure, respectively.

This paper uses a method (the so-called SIMPLE method [8]) providing a relation between the pressure and the velocity with a pressure field, guaranteeing that the continuity equation is satisfied. It results in solving an equation of the Poisson-type for the pressure [7].

To formulate the SIMPLE algorithm, we write the equation of conservation of the momentum of the system (1)—(3) with time discretization by the Euler scheme:

$$\frac{\rho^n \mathbf{u}_i^{n+1} - \rho^j \mathbf{u}_i^j}{\Delta t} + \frac{\partial}{\partial x_j}\left(\rho^n \mathbf{u}_i^{n+1} \mathbf{u}_j^n\right) = -\frac{\partial p^{n+1}}{\partial x_i} + \frac{\partial}{\partial x_j}\left(\tau_{ij}^{n+1}\right). \tag{5}$$

Here n is the solution at the previous iteration and j is the solution at the previous time step. To solve this equation, the pressure and the velocity are presented in the form

$$u_i^{n+1} = u_i^n + u_i^*, \tag{6}$$

$$p^{n+1} = p^n + \alpha_p(p^{n+1} - p^n) = p^n + \alpha_p \delta p^{n+1}. \tag{7}$$

Here $0 \leq \alpha_p \leq 1$ is a relaxation parameter. Substitution of the above expression into (5) yields

$$\frac{\rho^n u_i^{n+1} - \rho^j u_i^j}{\Delta t} + \frac{\partial}{\partial x_j}\left(\rho^n u_i^{n+1} u_j^n\right) = -\frac{\partial p^n}{\partial x_i} - \frac{\partial\left(\delta p^{n+1}\right)}{\partial x_i} + \frac{\partial}{\partial x_j}\left(\tau_{ij}^{n+1}\right). \tag{8}$$

Substitution of the first expression in (7) into (5) allows us to obtain a preliminary estimate of the velocity at the next step from the equation

$$\frac{\rho^n u_i^*}{\Delta t} + \frac{\partial}{\partial x_j}\left(\rho^n u_i^* u_j^n\right) - \frac{\partial}{\partial x_j}\left(\tau_{ij}^*\right) = \frac{\rho^j u_i^j}{\Delta t} - \frac{\partial p^n}{\partial x_i}. \tag{9}$$

The molecular and turbulent components of the shear stress tensor in (1)—(3), (5), (7) are calculated using u_i^* as well. At the second stage, the total speed is calculated at iteration $n+1$ using a pressure correction:

$$u_i^{n+1} = u_i^* - \Delta t \frac{\partial\left(\delta p^{n+1}\right)}{\partial x_i}. \tag{10}$$

The pressure correction itself is found from (10) if the continuity condition for u_i^{n+1} is satisfied. Thus, taking the derivative of both sides of the above equality, we obtain the following Poisson equation for the pressure:

$$\frac{\partial}{\partial x_i}\left(\frac{\partial\left(\delta p^{n+1}\right)}{\partial x_i}\right) = \frac{1}{\Delta t}\frac{\partial u_i^*}{\partial x_i}. \tag{11}$$

This iterative procedure allows obtaining velocity and pressure fields that satisfy the system (1)—(3).

Equation (5) uses a second-order upwind scheme called LUD [19] to discretize the convective terms, a second-order central-difference scheme to discretize the viscous terms, and the Adams-Bashforth scheme [7, 19] to discretize the time derivative. The resulting systems of algebraic equations are solved using an algebraic multigrid solver called AMG [20, 21, 22] (AMG method is implemented in LOGOS [22]).

3. Numerical experiments

To estimate the space and time resolution required to simulate the propagation of acoustic perturbations in a liquid medium, we consider the propagation of perturbations in a liquid medium from a harmonic source of oscillations. Let us solve the following problem of propagation of acoustic oscillations of sinusoidal waves along an infinite plate: The waves are generated at the left edge of a plate of length

$L = 2$ m with a frequency of 20 KHz and propagate to the right edge, where they attenuate due to the use of a highly sparse mesh.

Let us introduce the following notation: A — acoustic wave amplitude, λ — wavelength, $K = \frac{2\pi}{\lambda}$ — wavenumber, T — oscillation period calculated by the formula $T = \frac{\lambda}{c_0}$, c_0 — sound speed and $v(t) = \sin(2\pi ft)$ — a harmonic function. The oscillation frequency f must be much less than the wavelength $\lambda = c_0/f$, where c_0 is the sound speed generated by the source. For the waves to be considered acoustic, the mass source amplitude, A_q must be given so that $A_q \ll \rho c_0^3/f^2$ already at distances of about a wavelength from the source.

To generate waves on the left boundary, the velocity component U_x is given by the relation $U_x = A{\cdot}\sin(2\pi ft)$. This boundary condition corresponds to the solution of a problem of propagation of sinusoidal waves [23], which provides the generation of a sinusoidal wave packet with the least distortions at the input boundary.

The fluid oscillations are considered in a water medium with the following parameters: $\rho = 1000kg/m^3$ (density), $\mu = 0,001Pa \cdot s$ (viscosity), $c_0 = 1400m/s$ (sound speed in water). The wavelength in such conditions $\lambda = 0,07m$ and the period $T = 5e^{-5}$.

In the numerical simulation of the problem at a finite grid and time resolution, the wave amplitude will gradually decrease due to the effect of numerical diffusion on the solution. The amplitude decrease of the waves when they pass a certain distance shows the magnitude of the numerical diffusion, and, hence, the grid resolution and the time step.

In the propagation of acoustic oscillations, a major factor is the longitudinal partition of the grid or a parameter that determines the number of cells per wavelength λ. This parameter must be considered together with the time step, Δt. A large time step generates large numerical diffusion and may be insufficient for describing high-frequency oscillations [17]. Therefore, in the calculations it must be bounded from above by a value at which numerical diffusion is reasonable. Also, in practical calculations the time step is bounded from above by an additional criterion which depends on the stability of the numerical method. One of the goals of this study is to determine which of these criteria for the time step must be used earlier, as well as estimate the universal character of the criteria for a wide range of frequencies. In the case of unsteady flow, a sufficiently converging solution must be obtained at each iteration step; an important role in this is played by the number of iterations per step. If the solution does not converge in a given number of iterations, the error of the numerical method will increase with each iterative procedure.

The method for studying the effects of the above parameters on the numerical diffusion of the computational method is as follows: To determine the effect of one of the parameters on the solution, a series of calculations with various values of this parameter are carried out. In this case, the other parameters are fixed and small enough not to make a large contribution to the numerical diffusion that affects the solution. The effect on the solution is expressed in the attenuation coefficient of a wave when it passes a distance of its wavelengths:

$$\delta_n = 1 - \frac{A_{n+1}}{A_n}. \tag{12}$$

Calculation no.	Δx, m	$\Delta x/\lambda$	N_λ	N_{iter}	$\Delta t/T$
1	0,005	0,07	14	20	0,02
2	0,003	0,04	23	20	0,02
3	0,0023	0,033	30	20	0,02
4	0,0018	0,025	40	20	0,02
5	0,0013	0,0188	60	20	0,02
6	0,00088	0,0125	80	20	0,02

TABLE 1. Parameters of grid resolution analysis

Here n is the wave number starting from the left edge of the plate. Consider an average value, $\delta = < \delta_n >$. Obviously, the finer is the grid and the smaller the time step, the closer is the attenuation coefficient δ to zero.

The attenuation coefficient is considered acceptable if, due to the influence of numerical diffusion, the amplitude of a wave passing a distance of its wavelength does not decrease by more than 0.5%:

$$\delta_n \leq 0,5\%. \tag{13}$$

This criterion will be used to estimate all four criteria given above.

3.1. **Influence of grid resolution.** To estimate the acceptable horizontal cell size, we will perform a series of calculations with the same wave parameters: $A = 0.005m$, $\lambda = 0,07m$. In each of the calculations, the time step and the vertical size of the cells remain constant, but the horizontal size of the cells changes. Table 1 shows the parameters of the computational grids and the time step (column N_λ shows the number of cells per wavelength).

In all of the calculations, the number of internal iterations per step and the time step remained unchanged; these values are such that for a major parameter, Δx, their effect on numerical diffusion is negligible. This statement was made on the basis of a series of preliminary numerical experiments, which showed that these parameter values have a minimal effect on the overall numerical diffusion of the method. This is true for the time step Δt, which is taken small with respect to the wave period. The size of the cells along the horizontal axis varied from 0.00088 m to 0.005 m, which means 80 and 14 calculation cells per wavelength, respectively.

In the calculations, the plate length L comprises about 20 wavelengths. To obtain a statistically stable pattern of oscillations, the calculations were made up to time $\tau = 30 \cdot T$. As a result, the pressure distribution along the horizontal axis of the plate was obtained.

Let us analyze the calculations for various grid models. Figure 1 shows the pressure distribution along the plate. There is almost no attenuation in the oscillations. However, at a coarse grid resolution there is a pronounced shift in the acoustic waves, which indicates a large error in the oscillation period. The calculated wave shift coefficient is $(\tau(P_{\max n}) - \tau(P_{\max n-1}))/N_w$.

One can see that at the coarsest grid resolution the first wave shift is about 0.5%, and already for the tenth wave it is about 5%. At a grid resolution of 40 or more cells per wavelength, the shift in the acoustic waves has an acceptable error of about 0.2% percent of the initial wavelength.

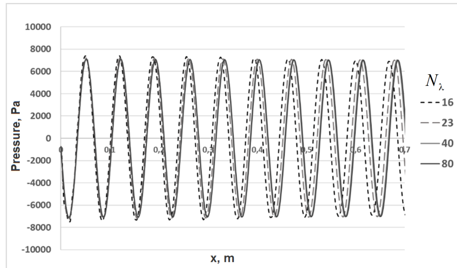

FIG. 1. Pressure oscillations along the plate for different numbers

Calculation no.	$\Delta x/\lambda$	N_λ	$\Delta\tau$, %	
1	0,005	0,07	14	0,47
2	0,003	0,04	23	0,28
3	0,0023	0,033	30	0,26
4	0,0018	0,025	40	0,21
5	0,0013	0,0188	60	0,20
6	0,00088	0,0125	80	0,19

TABLE 2. Results of grid resolution analysis

The shift for one wave in cases 4, 5, 6 remains at the same level and practically does not change when the number of cells per wavelength is doubled (see Table 2.

The results show that as Δx increases and, correspondingly, N_λ decreases, the shift increases to $\Delta\tau = 0,21\%$ for one wave, which means an increase in numerical diffusion. The calculation result with the largest value of Δx after which $\Delta\tau$ does not increase is shown by gray color in the table.

3.2. **Effect of the number of iterations for the nonlinear terms.** The acceptable number of internal iterations per time step in a non-stationary calculation is estimated by the same method. The frequencies of acoustic waves are assumed to be the same as in the previous case. The allowable number of internal iterations is estimated in the same way as in the study of the grid resolution for acoustic waves. In all calculations, the number of cells per wavelength and time step remained unchanged, and these values are such that, compared with the main parameter N_{iter}, their effect on numerical diffusion is insignificant.

The results presented in Table 3 show that the number of iterations per step greatly affects the pattern of acoustic perturbations: for instance, if the number of iterations per step is 5, the attenuation coefficient is 2.5%, which indicates a high level of numerical diffusion and insufficient convergence of the solution at the time step.

The results show that as Δx increases (and, hence, N_λ decreases) the shift increases to $\Delta\tau = 0,21\%$ for one wave, which means an increase in numerical diffusion. The calculation result with the largest value of Δx after which $\Delta\tau$ does not increase is shown by gray color in the table. Figure **??** shows pressure along the plate versus the number of internal iterations.

This series of calculations has shown that when choosing the grid size Δy_w the criterion associated with numerical diffusion is insignificant.

Calculation no.	N_λ	$\Delta t/T$	N_{iter}	δ, %	Comments
1	80	0,02	5	2,5	delay, with change in A
2	80	0,02	7	1	delay, with change in A
3	80	0,02	10	0,3	delay, with change in A
4	80	0,02	15	0,1	delay
5	80	0,02	20	0,05	
6	80	0,02	40	0,05	

TABLE 3. Results of analysis of the number of internal iterations

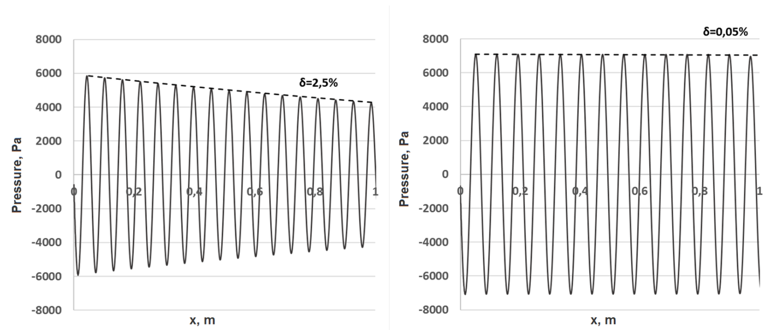

FIG. 2. Pressure oscillations along the plate and the envelope $\sigma(x)$ for different numbers of iterations per step: -5 (left), -20 (right)

Calculation no.	N_λ	N_{iter}	(%)T	δ, %
1	80	20	10	30
2	80	20	5	5
3	80	20	3,4	1,5
4	80	20	2	0,5
5	80	20	1	0,05
6	80	20	0,2	0,05

TABLE 4. Parameters of the fourth-step calculations

3.3. **Effect of time step size.** Taking into account the previous results obtained on a computational grid with the maximum number of cells per wavelength and an acceptable number of iterations per step, we estimate in a series of calculations the effect of the time step Δt on numerical diffusion by changing its value. Table 4 shows the calculation parameters and the obtained values of the attenuation coefficient δ.

The results show that the attenuation coefficient δ strongly depends on the time step Δt. According to (8), acceptable results are obtained only with time steps of $5e - 7$s, which corresponds to one percent of the oscillation period. Figure 3 shows pressure fluctuations along the plate for three values of the calculation step, illustrating that the damping of oscillations strongly depends on its values.

The results show that as the time step increases by more than 2% of the oscillation period, a significant attenuation of sound wave oscillations takes place, and the most acceptable time step value is 1% of the oscillation period. However, if multivariate calculations are needed, this parameter can be increased to 2%.

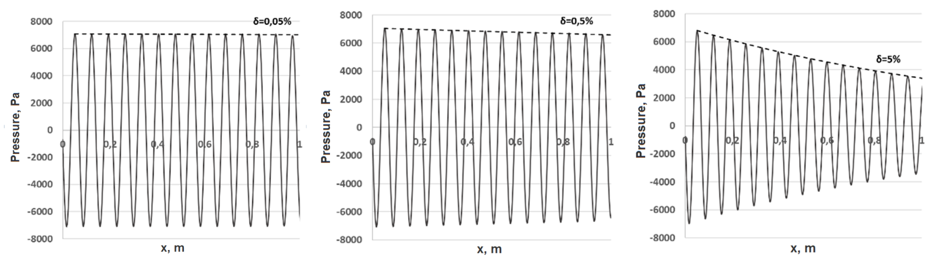

FIG. 3. Pressure fluctuations along the plate and shell for time steps: 0.2%T (left), 2%T (center), 5%T (right)

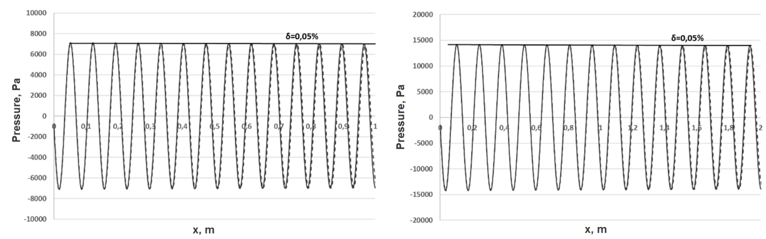

FIG. 4. Pressure oscillations along the plate and the envelope for 20 KHz (left), 10 KHz (right)

The purpose of this study is to assess the parameters of the numerical simulation of acoustic oscillations and the universal character of the above-proposed criteria. To confirm this fact, we will perform a numerical simulation of this problem using the most optimal of the criteria for two oscillation frequencies, 20 KHz and 10 KHz.

Figure 4 presents the results of the numerical simulation of acoustic oscillations of the different frequencies. The estimation measure will be the attenuation rate of an acoustic wave and its delay.

On the figure 4, the pressure distribution along the plate with the limit values of the parameters is shown by a dotted line, and the pressure distribution with the optimal parameters based on the above study is shown by a straight line. The time step was chosen so as to provide 1% of the oscillation period, the number of cells of the calculated area per wavelength was 40, and the number of internal iterations per step was 20. It can be seen that the use of optimal parameters does not introduce any numerical diffusion into the calculation method. It is also shown that the parameters are universal and can be used for different values of the frequency of the audio signal. The curves obtained using optimal parameters almost coincide with the curves with the limiting parameters of the problem.

3.4. **Simulation of perturbations from a point source.** To test the above method for calculating acoustic waves, consider a problem of propagation of acoustic oscillations with a frequency of 20 KHz from a point source.

In practice, it is difficult to numerically implement a point source, and in this problem the point source is given by the problem geometry. The radius of the source is taken equal to 0.1m, and the radius of the entire area is 7 m. The source

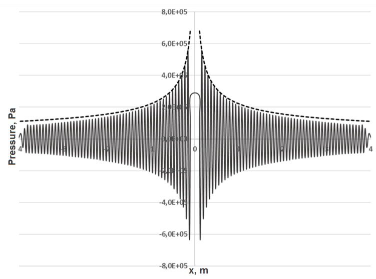

FIG. 5. Pressure oscillations along the domain and the envelope

amplitude is given as $A_q \ll \rho c_0^3/f^2$, so that the waves can be considered acoustic at distances of the order of the wavelength from the source. The waves are generated at a frequency of 20 kHz and propagate to the right border, where they attenuate due to the use of a highly sparse grid. The wave generation is given by a radial velocity relation $U_r = A \cdot \sin(2\pi f t)$. This boundary condition corresponds to the solution of a problem of propagation of sinusoidal waves [23], which provides the generation of a packet of sinusoidal waves in the radial direction.

The fluid oscillations are considered in a water medium with the following parameters: $\rho = 1000kg/m^3$ (density), $\mu = 0,001Pa \cdot s$ (viscosity), $c_0 = 1400m/s$ (sound speed in water). Under these conditions the wavelength $\lambda = 0,07m$ and the period $T = 5e^{-5}$.

We consider a compressible fluid with a compressibility coefficient calculated from a relationship between the pressure and density perturbations.

Figure 5 shows pressure oscillations along the calculation domain and the envelope. The calculation parameters are based on the above considerations

The oscillations from a point source must attenuate as $\sqrt{\frac{1}{R}}$. Figure 5 shows that the oscillations have the shape of the envelope and the attenuation takes place according to the law of $\sqrt{\frac{1}{R}}$.

4. Conclusions

In this study, estimates of the effects of various factors on the accuracy of numerical simulation of acoustic wave propagation have been obtained. It has been found that the number of cells per wavelength, $\Delta x/\lambda$, and the ratio of the time step to the acoustic wave period, $\Delta t/T$, have the largest effects. The number of internal iterations per time step has also an effect. The thus obtained quantitative criteria are as follows: the horizontal partition $N_\lambda \geq 40$; the number of iterations per time step $N_{iter} \geq 20$; the time step $\Delta t/T = 0,01$. Compliance with these criteria guarantees that the attenuation coefficient does not exceed a value of $\delta = 0,05$. This means that after passing a distance of 10 wavelengths the wave amplitude, due to the influence of numerical diffusion, decreases by no more than 0.5%. The results have been tested for various frequencies of acoustic oscillations on a problem with a harmonic oscillation source on a plate and a problem with a point source of oscillations. In future work we will compare the nonlinear effects of applying the direct problem solution based on the Navier-Stokes equations with linear hyperbolic system in application to acoustic tomography [33, 34, 36] and consider the effect of nonlinear effects on the data of the inverse problem.

References

[1] J.W. Strutt, *The Theory of Sound. Vol. I*, Macmillan, London, 1894. JFM 25.1604.01

[2] J.W. Strutt, *The Theory of Sound vol. II*, Macmillan, London, 1896. JFM 27.0701.05

[3] S. Kowalczyk, J. Felicjancik, *Numerical and experimental propeller noise investigations*, Ocean Engineering, **120** (2016), 108–115.

[4] N. Fukushima, K. Fukagata, N. Kasagi, H. Noguchi, K. Tanimoto, *Numerical and experimental study on turbulent thermal mixing in a T-junction flow*, The 6th ASME-JSME Thermal Engeneering Joint Conference, March 16-20, 2003.

[5] L.G. Loitsyanskii, *Mechanics of liquids and gases*, Pergamon Press, Oxford etc., 1972. Zbl 0247.76001

[6] S.H. Wasala, R.C. Storey, S.E. Norris, J.E. Cater, *Aeroacoustic noise prediction for wind turbines using Large Eddy Simulation*, Journal of Wind Engineering and Industrial Aerodynamics, **145** (2015), 17–29.

[7] J.H. Ferziger, M. Perić, *Computational methods for fluid dynamics*, Springer, Berlin, 2002. Zbl 0998.76001

[8] S.V. Lashkin, A.S. Kozelkov, A.V. Yalozo, V.Y. Gerasimov, D.K. Zelensky, *Efficiency analysis of the parallel implementation of the SIMPLE algorithm on multiprocessor computers*, J. Appl. Mech. Tech. Phy., **58**:7 (2017), 1242–1259.

[9] A.S. Kozelkov, S.V. Lashkin, V.R. Efremov, K.N. Volkov, Yu.A. Tsibereva, N.V. Tarasova, *An implicit algorithm of solving Navier–Stokes equations to simulate flows in anisotropic porous media*, Comput. Fluids, **160** (2018), 164–174. Zbl 1390.76462

[10] Z.J. Chen, A.J. Przekwas, *A coupled pressure-based computational method for incompressible/compressible flows*, J. Comput. Phys., **229**:24 (2010), 9150-9165. Zbl 1427.76200

[11] M. Cianferr, V. Armenio, S. Ianniello, *Hydroacoustic noise from different geometries*, Int. J. Heat Fluid flow, **70** (2018), 348–362.

[12] A. Inasawa, T. Nakano, M. Asai, *Development of wake vortices and the associated sound radiation in the flow past a rectangular cylinder of various aspect ratios*, 7th International Simposium on Turbulence and Shear Flow Phenomena, Ottava, Canada, July 27-31, 2011.

[13] A. Bodling, A. Sharm, *Numerical investigation of noise reduction mechanisms in a bio-inspired airfoil*, Journal of Sound and Vibration, **453** (2019), 314–327.

[14] A.V. Struchkov, A.S. Kozelkov, K. Volkov, A.A. Kurkin, R.N. Zhuchkov, A.V. Sarazov, *Numerical simulation of aerodynamic problems based on adaptive mesh refinement method*, Acta Astronautica, **172** (2020), 7–15.

[15] A.S. Kozelkov, O.L. Krutyakova, V.V. Kurulin, S.V. Lashkin, E.S. Tyatyushkina, *Application of numerical schemes with singling out the boundary layer for the computation of turbulent flows using eddy-resolving approaches on unstructured grids*, Comput. Math. Math. Phys., **57**:6 (2017), 1036–1047. Zbl 1457.76091

[16] A.S. Kozelkov, V.V. Kurulin *Eddy-resolving numerical scheme for simulation of turbulent incompressible flows*, Comput. Math. Math. Phys., **55**:7 (2015), 1232–1241. Zbl 1329.76140

[17] A.S. Kozelkov, V.V. Kurulin, S.V. Lashkin, R.M. Shagaliev, A.V. Yalozo, *Investigation of supercomputer capabilities for the scalable numerical simulation of computational fluid dynamics problems in industrial applications*, Comput. Math. Math. Phys., **56**:8 (2016), 1506–1516. Zbl 1445.76003

[18] A.S. Kozelkov, *The numerical technique for the landslide tsunami simulations based on Navier-Stokes equations*, J. Appl. Mech. Tech. Phy., **58**:7 (2017), 1192-1210.

[19] H. Jasak, *Error analysis and estimation for the finite volume method with applications to fluid flows*, Thesis submitted for the degree of doctor, Department of Mechanical Engineering, Imperial College of Science, 1996.

[20] K. Stüben, U. Trottenberg, *Multigrid methods: Fundamental algorithms, model problem analysis and applications*, Lect. Notes Math., **960**, Springer, 1982. Zbl 0505.65035

[21] Van Emden Henson, U. Meier-Yang, *Boomer AMG: A parallel algebraic multigrid solver and preconditioner*, Appl. Numer. Math., **41**:1 (2002), 155–177. Zbl 0995.65128

[22] K.N. Volkov, A.S. Kozelkov, S.V. Lashkin, N.V. Tarasova, A.V. Yalozo, *A parallel implementation of the algebraic multigrid method for solving problems in dynamics of viscous incompressible fluid*, Comput. Math. Math. Phys., **57**:12 (2017), 2030–2046. Zbl 1444.76045

[23] J.D. Fenton, *A fifth-order Stokes theory for steady waves*, Journal of Waterway Port Coastal and Ocean Engineering-asce, **111**:2 (1985), 216–234.

[24] S.K. Lele, *Compact finite difference schemes with spectral-like resolution*, J. Comput. Phys., **103**:1 (1992), 16–42. Zbl 0759.65006

[25] R. Jirik, I. Peterlik, N. Ruiter, J. Fousek, R. Dapp, M. Zapf, J. Jan, *Sound-speed image reconstruction in sparse-aperture 3-D ultrasound transmission tomography*, IEEE Trans. Ultrason. Ferroelectr. Freq. Control, **59**:2 (2012), 254–264.

[26] V.A. Burov, D.I. Zotov, O.D. Rumyantseva, *Reconstruction of the sound velocity and absorption spatial distributions in soft biological tissue phantoms from experimental ultrasound tomography data*, Acoust. Phys., **61**:2 (2015), 231–248.

[27] J. Wiskin, B. Malik, R. Natesan, M. Lenox, *Quantitative assessment of breast density using transmission ultrasound tomography*, Med. Phys., **46**:6 (2019), 2610–2620.

[28] M.V. Klibanov, *Travel time tomography with formally determined incomplete data in 3D*, Inverse Probl. Imaging, **13**:6 (2019), 1367–1393. Zbl 1427.35362

[29] M.V. Klibanov, *On the travel time tomography problem in 3D*, J. Inverse Ill-Posed Probl., **27**:4 (2019), 591–607. Zbl 1418.35375

[30] S.I. Kabanikhin, D.V. Klyuchinskiy, I.M. Kulikov, N.S. Novikov, M.A. Shishlenin, *Direct and inverse problems for conservation laws*, In *Continuum mechanics, applied mathematics and scientific computing: Godunov's legacy*, Springer, Cham, (2020), 217–222. MR4267117

[31] S.I. Kabanikhin, I.M. Kulikov, M.A. Shishlenin, *An algorithm for recovering the characteristics of the initial state of supernova*, Comput. Math. Math. Phys., **60**:6 (2020), 1008–1016. Zbl 1452.65209

[32] S.I. Kabanikhin, D.V. Klyuchinskiy, N.S. Novikov, M.A. Shishlenin, *Numerics of acoustical 2D tomography based on the conservation laws*, J. Inverse Ill-Posed Probl., **28**:2 (2020), 287–297. Zbl 1433.65196

[33] D. Klyuchinskiy, N. Novikov, M. Shishlenin, *A modification of gradient Descent method for solving coefficient inverse problem for acoustics equations*, Computation, **8**:3 (2020), 73.

[34] D. Klyuchinskiy, N. Novikov, M. Shishlenin, *Recovering density and speed of sound coefficients in the 2D hyperbolic system of acoustic equations of the first order by a finite number of observations*, Mathematics, **9**:2 (2021), 199.

[35] S.I. Kabanikhin, D.V. Klyuchinskiy, N.S. Novikov, M.A. Shishlenin, *On the problem of modeling the acoustic radiation pattern of source for the 2D first-order system of hyperbolic equations*, J. Physics: Conference Series, **1715**:1 (2021), Article ID 012038.

[36] D.V. Klyuchinskiy, N.S. Novikov, M.A. Shishlenin, *CPU-time and RAM memory optimization for solving dynamic inverse problems using gradient-based approach*, J. Comput. Physics, **439** (2021), Article ID 110374.

Andrey Sergeevich Kozelkov
Russian Federal Nuclear Center,
All-Russian Research Institute of Experimental Physics (FSUE RFNC-VNIIEF),
37, Mira ave.,
Sarov, Nizhny Novgorod region, 607188, Russia
Nizhny Novgorod State Technical University,
24, Minin str.,
Nizhny Novgorod, 603950, Russia
Moscow Aviation Institute (National Research University)
4, Volokolamskoe shosse,
Moscow, 125993, Russia
Email address: askozelkov@mail.ru

Olga Leonidovna Krutyakova
Russian Federal Nuclear Center,
All-Russian Research Institute of Experimental Physics (FSUE RFNC-VNIIEF),
37, Mira ave.,
Sarov, Nizhny Novgorod region, 607188, Russia
Email address: puch9@yandex.ru

Vadim Viktorovich Kurulin
Russian Federal Nuclear Center,
All-Russian Research Institute of Experimental Physics (FSUE RFNC-VNIIEF),
37, Mira ave.,
Sarov, Nizhny Novgorod region, 607188, Russia
Email address: kurulin@mail.ru

Dmitry Yurievich Strelets
Moscow Aviation Institute (National Research University)
4, Volokolamskoe shosse,
Moscow, 125993, Russia
Email address: dimstrelets@rambler.ru

Maxim Aleksandrovich Shishlenin
Institute of Computational Mathematics and Mathematical Geophysics,
6, Acad. Lavrent'yev ave.,
Novosibirsk, 630090, Russia
Novosibirsk State University,
1, Pirogova str.,
Novosibirsk, 630090, Russia
Email address: mshishlenin@ngs.ru